Phase diagram of the weak-coupling two-dimensional t-t' Hubbard model at low and intermediate electron density

Richard Hlubina
Department of Solid State Physics, Comenius University, Mlynská Dolina F2, 842 15 Bratislava, Slovakia
(Received 11 September 1998)

We study the stability of the ferromagnetic phase of the t-t' weak-coupling Hubbard model at low and intermediate electron density within the T-matrix approximation. The superconducting instability of the paramagnetic phase is discussed by a perturbative evaluation of the superconducting vertex.
[S0163-1829(99)11413-9]

I. INTRODUCTION

After the discovery of high-temperature superconductors, the interest in strongly correlated two-dimensional (2D) electron systems has risen substantially.[1] Initially, most studies concentrated on the simplest possible model compatible with the quantum chemistry of the cuprates, namely, a Hubbard (or t-J) model on a square lattice with electrons hopping only between nearest-neighbor sites of the lattice.[1,2] Recent photoemission experiments[3] indicate, however, that also longer-range hoppings are not negligible. The simplest model which produces a Fermi surface in qualitative agreement with experiments is

$$H=-t\sum_{\langle i,j\rangle,\sigma} c^{\dagger}_{i,\sigma}c_{j,\sigma}+t'\sum_{\langle\langle i,j\rangle\rangle,\sigma} c^{\dagger}_{i,\sigma}c_{j,\sigma}+U\sum_{i} n_{i,\uparrow}n_{i,\downarrow}, \tag{1}$$

where t and t' are the nearest-neighbor and next-nearest-neighbor hopping amplitudes, respectively. U is on-site electron-electron repulsion and $\langle i,j\rangle,\langle\langle i,j\rangle\rangle$ are pairs of nearest and next-nearest neighbors. The noninteracting Fermi line of the model Eq. (1) resembles that observed experimentally in the cuprates for $t'/t>0$.

The parameter region of Eq. (1) relevant for the cuprates, namely electron density per lattice site $0.75<\rho\leqslant 1,0<R=2t'/t<1$, and $U/t\sim 8$, turned out to be difficult to analyze.[4] In this paper, we address a less ambitious question: What is the phase diagram of Eq. (1) at low and intermediate electron density at moderate coupling? In addition to being interesting in its own right, we believe that a solid understanding of the intermediate-density range might help attacking the high-T_c problem from the overdoped side.

The outline of the paper is as follows. In Sec. II, we elaborate on the recent observation[5] that the t-t' Hubbard model Eq. (1) exhibits, for $R\sim 1$, an itinerant ferromagnetic phase at the Van Hove density. The latter is defined as that density, for which the Fermi line of the noninteracting problem crosses the saddle points of the bare electron spectrum

$$\varepsilon_{\mathbf{k}}=-2t(\cos k_x+\cos k_y)+4t'\cos k_x\cos k_y, \tag{2}$$

which are at $(\pi,0)$ and $(0,\pi)$ for $|R|<1$. In Ref. 5, good agreement was found between the predictions of the T-matrix approximation (TMA) and quantum Monte Carlo simulations of clusters with up to 16×16 sites. On the other hand, recent studies of the t-t' Hubbard model have found a finite window of densities around the Van Hove density where ferromagnetism is stabilized.[6,7] Motivated by these results we have performed a detailed study of the stability of the ferromagnetic phase at low and intermediate electron density within TMA.

In Sec. III we pursue an analogy to the physics of liquid ^{3}He: in the paramagnetic phase of the t-t' Hubbard model, ferromagnetic fluctuations should increase when approaching the ferromagnetic phase, and this in turn should lead to superconducting pairing in the p-wave channel.[8] Thus Eq. (1) might be an ideal toy model for the study of triplet superconductivity. As a first step in this direction, we determine the symmetry of the leading superconducting instability throughout the paramagnetic part of the phase diagram. This is done by a perturbative evaluation of the superconducting vertex, following the pioneering work of Kohn and Luttinger.[9] Recently, a similarly motivated study of the superconducting phase diagram of the t-t'-J model has appeared,[10] but our discussion is technically quite different.

The superconducting phase diagram of the model Eq. (1) might be relevant also to the compound Sr_2RuO_4, in which superconductivity has been found near 1 K. In fact, Sr_2RuO_4 is a quasi-2D compound isostructural to the high-temperature superconductor La_2CuO_4. The four d electrons per each Ru^{4+} ion fill three overlapping conduction bands α,β (of mixed d_{xz} and d_{yz} character), and γ (of d_{xy} character). Sr_2RuO_4 is believed to be a p-wave superconductor.[11,12] It has been argued that the superconducting coupling between the α,β bands and the γ band is weak.[13] Moreover, recent NMR experiments indicate that also the magnetic coupling between the d_{xz} and d_{yz} orbitals and the d_{xy} orbitals is small and the spin susceptibility is more enhanced for the γ band.[14] Therefore it is tempting to describe the superconductivity of Sr_2RuO_4 as being driven by the pairing instability of the γ band. Simple quantum chemistry considerations suggest that the γ band is described by the model Eq. (1).

II. MAGNETIC PHASE DIAGRAM

We consider clusters with $\Omega=L\times L$ sites and periodic boundary conditions. Only those electron fillings $N=N_{\uparrow}+N_{\downarrow}$, for which both N_{σ} (where $\sigma=\uparrow,\downarrow$) correspond to closed energy shells are considered. For given $N_{\uparrow}$ and $N_{\downarrow}$,

we calculate the ground-state energy from

$$E=\sum_{\mathbf{k},\sigma} f_\sigma(\mathbf{k})\varepsilon_{\mathbf{k}}+\frac{U}{\Omega}\sum_{\mathbf{k},\mathbf{k}'}\frac{f_\uparrow(\mathbf{k})f_\downarrow(\mathbf{k}')}{1+U\chi_{\rm pp}(\mathbf{k}+\mathbf{k}',\tilde{\varepsilon}_{\mathbf{k},\uparrow}+\tilde{\varepsilon}_{\mathbf{k}',\downarrow})}, \tag{3}$$

where $f_\sigma(\mathbf{k})$ is the distribution function for the noninteracting system, $\tilde{\varepsilon}_{\mathbf{k},\sigma}=\varepsilon_{\mathbf{k}}-\mu_\sigma$, μ_σ is the Fermi energy for electrons with spin σ, and

$$\chi_{\rm pp}(\mathbf{q},\omega)=\frac{1}{\Omega}\sum_{\mathbf{p}}\frac{[1-f_\uparrow(\mathbf{p})][1-f_\downarrow(-\mathbf{p}+\mathbf{q})]}{\tilde{\varepsilon}_{\mathbf{p},\uparrow}+\tilde{\varepsilon}_{-\mathbf{p}+\mathbf{q},\downarrow}-\omega}$$

is a particle-particle susceptibility. We calculate the ground-state energy E for all closed-shell partitions of N and identify the paramagnetic state with the case when the minimum of E is achieved for the minimal possible $|N_\uparrow-N_\downarrow|$. The above method for determining the stability of the paramagnetic state has been used long ago by Kanamori[15] and we shall refer to it as TMA, although a more correct name would be ''low-density approximation.'' In fact, the ground-state energy in the full T-matrix approximation reads

$$E_{\rm TMA}=\sum_{\mathbf{k},\sigma} f_\sigma(\mathbf{k})\varepsilon(\mathbf{k})-\frac{U}{2}(1-n)+\sum_{\mathbf{q}}\int_0^\infty\frac{d\omega}{2\pi}\ln[(1+U\chi_1)^2+(U\chi_2)^2], \tag{4}$$

where $\chi_1+i\chi_2=\chi_{\rm pp}(\mathbf{q},i\omega)-\chi_{\rm hh}(\mathbf{q},i\omega)$ and

$$\chi_{\rm hh}(\mathbf{q},\omega)=\frac{1}{\Omega}\sum_{\mathbf{p}}\frac{f_\uparrow(\mathbf{p})f_\downarrow(-\mathbf{p}+\mathbf{q})}{\tilde{\varepsilon}_{\mathbf{p},\uparrow}+\tilde{\varepsilon}_{-\mathbf{p}+\mathbf{q},\downarrow}-\omega}$$

is a hole-hole susceptibility. Equation (4) has been used in Ref. 5 and good agreement with quantum Monte Carlo simulations has been found there. We have checked Eq. (3) against the numerical data in Ref. 5 and found, surprisingly, that it works even better than Eq. (4). Nevertheless, the difference between the two calculations is less than 1%. This is because, in the low-density limit, the contribution of virtual processes with excited pairs of holes [which are included in Eq. (4) but not in Eq. (3)] is negligible. In what follows, we shall therefore identify Eq. (3) with TMA.

The region of stability of the fully polarized (Nagaoka) state against the paramagnetic state of the t-t' Hubbard model, determined numerically from Eq. (3) in the region $0<R<1$ for $U=4t$ and $U=8t$, is shown in Figs. 1 and 2, respectively. It is seen that at finite U, there is a finite window of densities around the Van Hove density, where the Nagaoka state is stable. The size of this window grows with U.

Also shown in Figs. 1 and 2 is a comparison of our TMA results to variational estimates of the region of stability of the Nagaoka state against single spin flips. The simplest nontrivial variational wave function,[16]

$$|\psi\rangle=\prod_i(1-\eta n_{i,\uparrow}n_{i,\downarrow})c^\dagger_{\mathbf{k}=0,\downarrow}|N-1\rangle, \tag{5}$$

is chosen for that purpose, with $|N-1\rangle$ being a Nagaoka state with $N-1$ spin-up electrons and a variational parameter η. This wave function has been applied to the model Eq. (1) in Refs. 17 and 6. The shape of the fully polarized ferromagnetic region determined from Eq. (5) is qualitatively similar to the TMA prediction, with an important exception in the limit $\rho\to0$: TMA predicts that in this limit, the paramagnet is stable for all $R<1$ at any U, whereas it can be shown by the methods introduced in Ref. 6 that according to Eq. (5), for all $R_c<R<1$ there exists

$$U_c=\frac{4\pi(2-R)(1-R)}{(\pi-1)R-(\pi-2)}$$

such that for $U>U_c$, Nagaoka ferromagnetism extends down to $\rho=0$. For $R<R_c=(\pi-2)/(\pi-1)$, Nagaoka ferromagnetism cannot be stabilized at $\rho\to0$. Our TMA results should be superior to those obtained from the variational ansatz Eq. (5) in the limit $\rho\to0$.

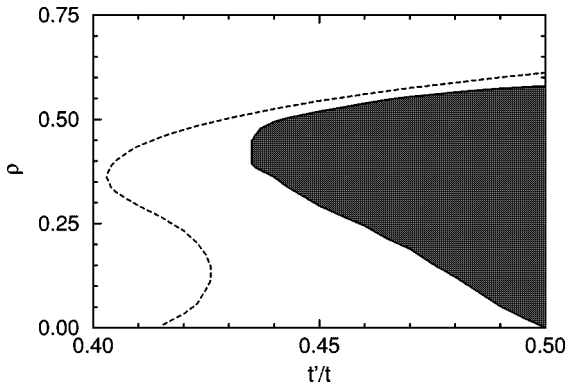

FIG. 1. Phase diagram at $U=4t$. Shaded area: region of stability of the fully polarized state (in TMA, $L=32$). Dashed line: boundary of the region where the Nagaoka state is stable against the single spin flip state Eq. (5).

We have tested the effect of the finite size of the lattice used in the calculation of the TMA phase diagram Fig. 1 on the location of the low-density phase boundary for $t'/t=0.495$, where the effect of finite L is expected to be largest, due to the small size of the Fermi surface at low density. Lattices with up to $L=200$ have been studied. It was found that the critical density for ferromagnetism for $L=32$ deviates less than 10% from the $L=200$ result.

In Fig. 3 we present energy vs magnetization curves $E(m)$ for electron densities close to the paramagnet-ferromagnet phase boundary. For clarity, the energy of the

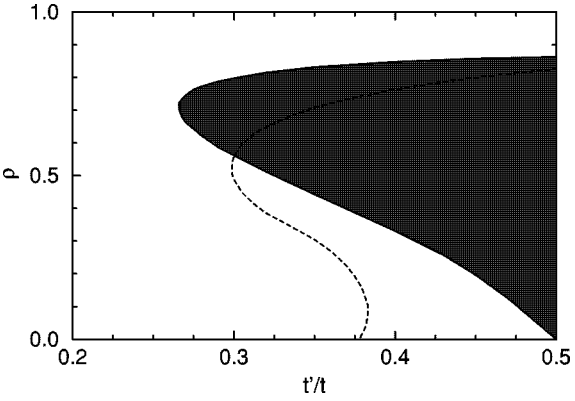

FIG. 2. The same as in Fig. 1, but for $U=8t$.

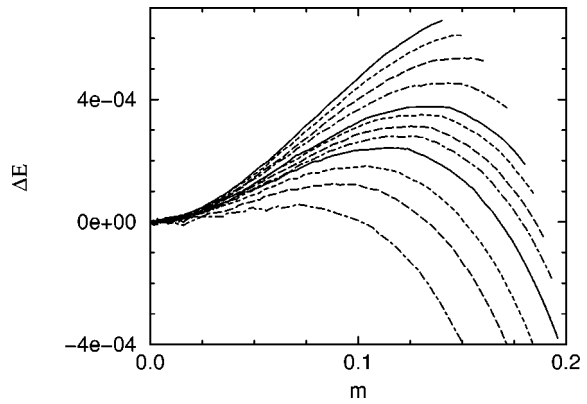

FIG. 3. $\Delta E = E(m) - E(0)$ (per site, in units of t) vs magnetization $m = (N_\uparrow - N_\downarrow)/\Omega$ for $t'/t = 0.47$ and $U = 4t$ in TMA, $L = 100$. The curves from top to bottom correspond to N = 1402, 1506, 1602, 1714, 1802, 1842, 1890, 1930, 2002, 2106, 2210, and 2402.

paramagnetic state $E(0)$ has been subtracted from the data. It is seen from here that the origin of the ferromagnetic phase shown in Fig. 1 is not in a weak-coupling instability of the paramagnetic phase, but rather in a level crossing between a paramagnetic and a fully polarized state.

On the other hand, close to the Van Hove density but outside the region of stability of the Nagaoka state, we find that partially polarized ferromagnetic states are stabilized. An example is presented in Fig. 4, where energy vs magnetization $E(m)$ (normalized to 0 for $m = 0$ as in Fig. 3) is shown for a system at the Van Hove density with $t'/t = 0.44$ and $U = 4t$. This is an example of a weak-coupling instability of the paramagnetic phase, which has been predicted for the model Eq. (1) at the Van Hove density in Ref. 5. Note that the agreement between the data for $L = 48$ and $L = 100$ suggests that the $L = 100$ data is essentially already in the thermodynamic limit.

For the first-order paramagnet-ferromagnet transition at fixed R as a function of ρ shown in Fig. 3, we expect (in absence of long-range Coulomb interactions) phase separation into a paramagnetic and a fully polarized state with different densities. In Fig. 5 we plot the TMA energy of the paramagnet and of the Nagaoka state vs ρ for $L = 32$. By Maxwell construction, we find phase separation for $0.174 < \rho < 0.197$ and $0.521 < \rho < 0.584$. In the inset, we show the difference ΔE between the energies of the paramagnet and of the Nagaoka state vs ρ at low densities for $L = 32$ and $L = 100$. Note that the TMA calculation of $\Delta E(\rho)$ is essentially converged already at $L = 32$. In fact, from the $L = 100$ data we find the low-density phase separation for $0.177 < \rho < 0.200$, quite close to the estimate for the 32×32 lattice.

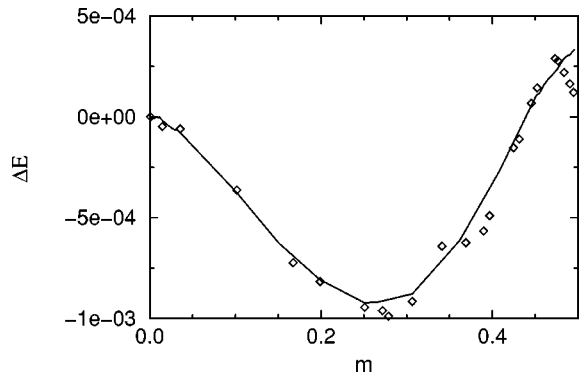

FIG. 4. $\Delta E = E(m) - E(0)$ (per site, in units of t) vs magnetization m for $t'/t = 0.44$ and $U = 4t$ in TMA. Solid line: $L = 100$. Diamonds: $L = 48$. $N = 4956$ ($N = 1140$) corresponds to the Van Hove density for $L = 100$ ($L = 48$).

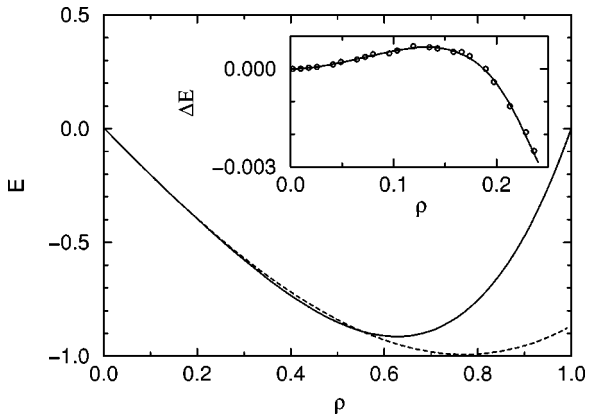

FIG. 5. Energy per site in units of t vs electron density $\rho = N/\Omega$ for $t'/t = 0.47$ and $U = 4t$ in TMA, $L = 32$. Full line: Nagaoka state. Dashed line: paramagnetic state. The inset shows $\Delta E = E_{\text{Nagaoka}} - E_{\text{paramagnet}}$ (per site, in units of t) vs electron density for the same parameters. The lattice sizes are $L = 100$ (full line) and $L = 32$ (circles).

Figure 4 shows that it is not true (at least within TMA) that the instability of the Nagaoka state against single spin flips implies a paramagnetic phase. On the other hand, Fig. 3 illustrates that neither the assumption that a locally stable Nagaoka state implies a stable ferromagnetic phase needs to be true. These two findings might put some doubts on the validity of estimates of the stability of ferromagnetism from the stability of the Nagaoka state against spin flips. However, we find that these anomalies (and also phase separation between the paramagnetic and the fully polarized states) occur in the t-t' Hubbard model only close to the phase boundary and neglecting them does not lead to significant changes of the phase diagram.

III. BCS INSTABILITY OF THE PARAMAGNETIC PHASE

Kohn and Luttinger[9] argued that even a purely repulsive degenerate Fermi system such as He^3 can be unstable towards pairing. They evaluated the Cooper-channel vertex to second order in the interaction and showed that, for a rotationally invariant 3D system with a hard-core repulsion, the system is unstable towards superconductivity with large odd angular momentum l of the Cooper pairs. Later it was shown that even at $l = 1$ pairing is favorable for this system,[18] in agreement with the p-wave symmetry of the pairing state in ^{3}He.[8] The latter has also been interpreted as being due to an exchange of magnetic fluctuations which play the role of phonons in conventional superconductors.[8] It is interesting to note that the superconducting vertex in the Kohn-Luttinger argument can be viewed as the lowest-order nontrivial term (in an expansion in powers of U) of a vertex arising from an exchange of magnons.

Superconducting instabilities of 3D lattice systems with

spin or charge susceptibilities enhanced at *finite* wave vectors have been studied within a similar fluctuation-exchange scheme.[19] After the discovery of superconductivity in the cuprates, it was quickly established that for the relevant case of a nearly half filled 2D electron band with repulsive interactions,[1,2] the fluctuation-exchange scheme predicts *d*-wave symmetry of their superconducting state.[20] We shall see below that, as was the case for ^{3}He, the Kohn-Luttinger effect predicts the same symmetry of the superconducting state as the fluctuation-exchange approximation. Remarkably, there is substantial experimental evidence for the *d*-wave symmetry of the pairing state in the cuprates.[21]

The above examples indicate that the Kohn-Luttinger method is a reasonable tool for estimating the symmetry of the leading superconducting instability. In this section we shall apply it to the superconducting phase diagram of the model Eq. (1). Chubukov and Lu[22] studied this problem in the limit of vanishing electron density ρ. Here we extend their discussion to finite ρ.

Let us analyze first the possible symmetries of the superconducting gap function $\Delta(\mathbf{k})$.[21] There are five irreducible representations of the point group of the square lattice. The four one-dimensional representations are even under inversion and correspond to singlet superconductivity.[23] We shall denote them s,d,d_{xy}, and g. Basis functions belonging to s that are not constant are usually called extended s in the literature, but we shall not make this distinction here. d is a shorthand notation for $d_{x^2-y^2}$. The two-dimensional representation p is odd under inversion and corresponds to triplet states.[23]

Let φ denote the angle between the vector connecting a given point on the Fermi line with the center of the Fermi line [which is (0,0) or (π,π), depending on ρ] and the k_x direction. Then in every symmetry sector α $(=s,d,d_{xy},g,p)$ we can expand the gap function in a series:

$$\Delta_\alpha(\varphi)=\sum_{n=0}^{\infty} c_n g_{\alpha,n}(\varphi), \tag{6}$$

where we have chosen the following basis functions $g_{\alpha,n}$:

$$g_{s,n}(\varphi)=N_n(\varphi)\cos[4n\varphi],$$

$$g_{d,n}(\varphi)=N_1(\varphi)\cos[(4n+2)\varphi],$$

$$g_{dxy,n}(\varphi)=N_1(\varphi)\sin[(4n+2)\varphi],$$

$$g_{g,n}(\varphi)=N_1(\varphi)\sin[4n\varphi],$$

$$g_{p,n}(\varphi)=N_1(\varphi)\times\begin{cases}\sin[(2n+1)\varphi]\\ \cos[(2n+1)\varphi].\end{cases}$$

The normalization factors $N_n(\varphi)=\sqrt{(2-\delta_{n,0})/D(\varphi)}$, where $D(\varphi)=(2\pi/v)(dk/d\varphi)$ is the angle-resolved density of states, are chosen so that

$$\oint \frac{dk}{v_{\mathbf{k}}} g_{\alpha,n}(\mathbf{k}) g_{\beta,m}(\mathbf{k})=\delta_{\alpha,\beta}\delta_{n,m}.$$

The effective interaction in the Cooper channel $V(\mathbf{k},\mathbf{k}')$ is given, to second order in U, by the diagram (d) in Fig. 1 of Ref. 9. Let us introduce the particle-hole susceptibility

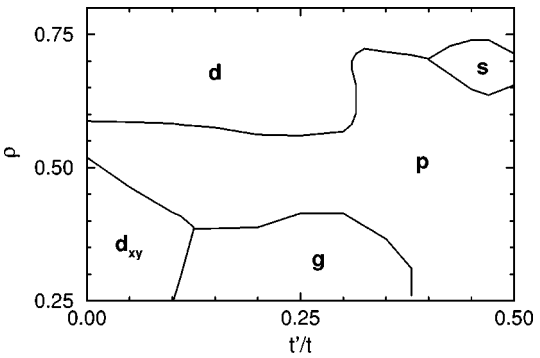

FIG. 6. Superconducting phase diagram for $U\to 0$. A small region of d_{xy}-wave (p-wave) pairing close to the s/p (d_{xy}/g) boundary is not displayed.

$$\chi(\mathbf{q})=\sum_{\mathbf{k}} \frac{f_{\mathbf{k}+\mathbf{q}}-f_{\mathbf{k}}}{\varepsilon_{\mathbf{k}}-\varepsilon\mathbf{k}+\mathbf{q}}. \tag{7}$$

Then $V(\mathbf{k},\mathbf{k}')=U+U^2\chi(\mathbf{k}+\mathbf{k}')$ and the BCS coupling constant in the symmetry sector α is[19]

$$\lambda_\alpha=-\frac{\oint \frac{dk}{v_{\mathbf{k}}}\oint \frac{dk'}{v_{\mathbf{k}'}} V(\mathbf{k},\mathbf{k}')\Delta_\alpha(\mathbf{k})\Delta_\alpha(\mathbf{k}')}{(2\pi)^2\oint \frac{dk}{v_{\mathbf{k}}}\Delta_\alpha(\mathbf{k})^2}. \tag{8}$$

Let us restrict the sum in Eq. (6) to $0\leqslant n\leqslant\mathcal{N}$. Then

$$\lambda_\alpha=-\frac{\sum_{n=0}^{\mathcal{N}}\sum_{m=0}^{\mathcal{N}} V^\alpha_{n,m}c_n c_m}{\sum_{n=0}^{\mathcal{N}} c_n^2}, \tag{9}$$

where

$$V^\alpha_{n,m}=(2\pi)^{-2}\oint (dk/v_{\mathbf{k}})\oint (dk'/v_{\mathbf{k}'})V(\mathbf{k},\mathbf{k}')\times g_{\alpha,n}(\mathbf{k})g_{\alpha,m}(\mathbf{k}')$$

is a real symmetric $\mathcal{N}\times\mathcal{N}$ matrix. It follows from Eq. (9) that the maximal superconducting coupling constant for a given α is $\lambda_\alpha=\max\{-\lambda_{\alpha,i}\}$, where $\lambda_{\alpha,i}$ are the eigenvalues $i=1,\ldots,\mathcal{N}$ of $V^\alpha_{n,m}$.

In Fig. 6 we show the superconducting phase diagram calculated numerically from Eq. (9). We have considered $\mathcal{N}=15$ harmonics in every symmetry sector α. All λ_α were attractive basically in the whole studied phase space. The susceptibility Eq. (7) was evaluated at a finite temperature $T=0.003t$.[24] This introduces only insignificant difference with respect to $T=0$, except for the case of $\rho\to 0$. In that limit, the electron spectrum becomes isotropic, $\chi(q)=m/2\pi$ for all $q\leqslant 2k_F$ at $T=0$, and the lowest-order Kohn-Luttinger effect vanishes at $T=0$.[22] However, at a finite temperature,

$$\chi(q)=\frac{m}{4\pi}\int_0^{\omega_q}\frac{d\varepsilon f(\varepsilon-\mu)}{\sqrt{\omega_q(\omega_q-\varepsilon)}},$$

where $\omega_q = q^2/8m$. The Fermi energy $\mu = k_F^2/2m$ and ε are measured here from the bottom of the band. For $T \ll \mu$, we still have $\chi(q) \approx m/2\pi$, but for $2k_F - T/v_F < q < 2k_F$, $\chi(q) \approx m/2\pi - \delta\chi$, where $\delta\chi \sim (m/2\pi)\sqrt{T/\mu}$. Thus evaluating $\chi(\mathbf{q})$ at $T>0$ leads to a nonzero Kohn-Luttinger effect [see Eq. (8)] even for an isotropic spectrum, with $\lambda \sim m^3 U^2 T/\rho$ in all symmetry sectors [provided $\oint dk \Delta(\mathbf{k}) = 0$]. Our calculation is therefore valid only in the region of densities where, at $T=0$, the modulation $\delta\chi$ of $\chi(\mathbf{q})$ for those values of $\mathbf{q}$ which span the Fermi line ($q \leqslant 2k_F$ in the isotropic case) is larger than thermal effects, $\delta\chi/\chi \gg \sqrt{T/\mu}$. For $T = 0.003t$ we restrict ourselves to $\rho > 0.25$.

As a function of ρ at fixed R and U, the maximal coupling constant $\max_\alpha(\lambda_\alpha)$ scales roughly with the density of states at the Fermi energy. Figure 6 shows that close to half filling ($\rho = 1$), d-wave pairing is the largest one for all $0 \leqslant R \leqslant 1$. In the low-density region, we find dominant d_{xy}-wave pairing for $R < 0.2$ and p-wave pairing for $R > 0.76$,[25] while at intermediate R, g-wave pairing dominates. This is consistent with Ref. 22.

The phase diagram is quite rich, since all allowed symmetry sectors are realized in its various parts. Its perhaps most unexpected features are the stability of the p-wave pairing at $\rho \approx 0.55$ for all $0 \leqslant R \leqslant 1$ and the small region of s-wave pairing around $\rho \approx 0.7$ and $R \approx 0.9$.

We emphasize that Fig. 6 is not a $T=0$ phase diagram. Its actual meaning is the following: for each point in the R-ρ plane, we assume that a superconducting state develops as the temperature is lowered below some $T_c(R,\rho)$. In Fig. 6, we plot the symmetry of the superconducting state for each point (R,ρ) at a temperature infinitesimally below $T_c(R,\rho)$. This symmetry is well defined away from the phase boundaries in Fig. 6. Exactly at the phase boundary, states of mixed symmetry may occur.[26] If the temperature lowers further below $T_c(R,\rho)$, states of mixed symmetry may develop in a subset of the R-ρ plane with nonzero measure. This question shall not be addressed in this paper.

Finally, let us note that the results shown in Fig. 6 are valid only in the limit $U \to 0$. Nevertheless, for finite U when also magnetic phases are stabilized (see Figs. 1 and 2), we hypothesize a similar pattern of the leading pairing instabilities of the paramagnetic phase.

IV. CONCLUSIONS

Within TMA, we have found that the t-t' Hubbard model supports a wide region of ferromagnetism around the Van Hove density, whose size grows with increasing U. In the same approximation we find that local instability (stability) of the Nagaoka state does not imply paramagnetism (ferromagnetism). However, our results indicate that these implications are broken only close to the paramagnet-ferromagnet phase boundary. This indicates that the single spin flip criterion widely used in the study of the stability of metallic ferromagnetism[16,6] provides reasonable estimates of the magnetic phase diagram.

In one dimension, the model Eq. (1) has been studied by many authors starting by Ref. 27, where it was shown that Nagaoka's proof of ferromagnetism applies for one hole in the half filled system, if $t'/t > 0$. A detailed review of recent work on the 1D model can be found in Ref. 28. The conclusion is that also in one dimension there is a large region of ferromagnetism in the ρ vs t'/t plane, if $0 < \rho < 1$ and $t'/t > 0$. On the other hand, ferromagnetism is stable within dynamical mean-field theory[29] on both 3D and $D=\infty$ fcc lattices in a wide range of fillings. Note that since there is a close connection between the t-t' model and an fcc lattice, it seems to be well established now that ferromagnetism in the t-t' Hubbard model is a robust phenomenon. It has been hypothesized that this is due to the asymmetric density of states of the model Eq. (1) with a large peak close to the band edge.[6,30] Although our results are consistent with this hypothesis, further work is needed to confirm it.

As regards the t-t' Hubbard model as a paradigm for magnon induced p-wave superconductivity, its main advantage is that the ferromagnetic phase appears at moderate values of U, where quantum Monte Carlo simulations could be feasible. The obvious alternative of studying the $t'=0$ model close to half filling, in the proximity of Nagaoka ferromagnetism, is an inherently strong-coupling problem.[31] The latter (for $U \to \infty$) has been studied so far only by slave-boson methods,[32] with the somewhat disappointing result that close to half filling, superconductivity appears in the d_{xy} channel.

Let us close by discussing the relevance of our data to Sr_2RuO_4. The Fermi surface of the γ band is well described by Eq. (2) with $t'/t \approx -0.3$ and $\rho \approx 1.33$.[33,34] By particle-hole symmetry, this is equivalent to $t'/t \approx 0.3$ and $\rho \approx 0.67$, which is close to the p-wave region in Fig. 6. Therefore superconductivity in Sr_2RuO_4 might be driven by the p-wave instability of the γ band.

ACKNOWLEDGMENTS

I thank S. Sorella for stimulating discussions and D. F. Agterberg and T. M. Rice for introducing me to the physics of Sr_2RuO_4. Part of this work was performed at the Institut für Theoretische Physik, Eidgenössische Technische Hochschule Zürich. Support by Slovak Grant Agency Grant No. 1/4300/97 and Comenius University Grant No. UK/3927/98 is acknowledged.

[1] For a comprehensive description of the physics of the cuprates from this point of view, see P.W. Anderson, *The Theory of Superconductivity in the High-T_c Cuprates* (Princeton University Press, Princeton, NJ, 1997).

[2] F.C. Zhang and T.M. Rice, Phys. Rev. B **37**, 3759 (1988).

[3] For a review, see M. Randeria and J.C. Campuzano, cond-mat/9709107 (unpublished).

[4] C. Buhler and A. Moreo, cond-mat/9807034 (unpublished), and references therein.

[5] R. Hlubina, S. Sorella, and F. Guinea, Phys. Rev. Lett. **78**, 1343 (1997).

[6] T. Hanisch, G.S. Uhrig, and E. Müller-Hartmann, Phys. Rev. B **56**, 13 960 (1997).

[7] M. Fleck, A.M. Oleś, and L. Hedin, Phys. Rev. B **56**, 3159

(1997).
[8] See, e.g., P.W. Anderson, *Basic Notions of Condensed Matter Physics* (Addison-Wesley, Redwood City, 1984).
[9] W. Kohn and J.M. Luttinger, Phys. Rev. Lett. **15**, 524 (1965).
[10] B.E.C. Koltenbah and R. Joynt, Rep. Prog. Phys. **60**, 23 (1997).
[11] T.M. Rice and M. Sigrist, J. Phys.: Condens. Matter **7**, L643 (1995).
[12] For a recent discussion of the pairing symmetry in Sr_2RuO_4, see D.F. Agterberg, Phys. Rev. Lett. **80**, 5184 (1998).
[13] D.F. Agterberg, T.M. Rice, and M. Sigrist, Phys. Rev. Lett. **78**, 3374 (1997).
[14] T. Imai, A. W. Hunt, K. R. Thurber, and F. C. Chou, Phys. Rev. Lett. **81**, 3006 (1998).
[15] J. Kanamori, Prog. Theor. Phys. **30**, 275 (1963).
[16] B.S. Shastry, H.R. Krishnamurthy, and P.W. Anderson, Phys. Rev. B **41**, 2375 (1990).
[17] P. Pieri, S. Daul, D. Baeriswyl, M. Dzierzawa, and P. Fazekous, Phys. Rev. B **54**, 9250 (1996).
[18] M.Yu. Kagan and A.V. Chubukov, JETP Lett. **50**, 517 (1989).
[19] D.J. Scalapino, E. Loh, and J.E. Hirsch, Phys. Rev. B **34**, 8190 (1986); **35**, 6694 (1987).
[20] For a review, see D.J. Scalapino, Phys. Rep. **250**, 329 (1995).
[21] For a review, see J. Annett, N. Goldenfeld, and A.J. Leggett, in *Physical Properties of High Temperature Superconductors V*, edited by D.M. Ginsberg (World Scientific, Singapore, 1996).
[22] A.V. Chubukov and J.P. Lu, Phys. Rev. B **46**, 11 163 (1992).
[23] We do not consider odd-frequency pairing, where even (odd) parity implies triplet (singlet) pairing (Ref. 21).
[24] At a given T, the thermodynamic limit of Eq. (7) is achieved only for a lattice size $L > L_c \propto T^{-1}$. In Fig. 6 we have used $L = 600$. The phase diagram calculated for $L = 400$ is essentially identical. Thus we expect $L_c \sim 400$.
[25] Estimates for $\rho = 0.25$.
[26] G. Kotliar, Phys. Rev. B **37**, 3664 (1988).
[27] D.C. Mattis and R.E. Peña, Phys. Rev. B **10**, 1006 (1974).
[28] S. Daul and R.M. Noack, Phys. Rev. B **58**, 2635 (1998).
[29] M. Ulmke, Eur. Phys. J. B **1**, 301 (1998).
[30] D. Vollhardt, N. Blümer, K. Held, M. Kollar, J. Schlipf, and M. Ulmke, Z. Phys. B **103**, 283 (1997).
[31] The Nagaoka state is unstable against single spin flip states for $U/t < 77.7$; see P. Wurth, G.S. Uhrig, and E. Müller-Hartmann, Ann. Phys. (Leipzig) **5**, 148 (1996).
[32] G. Kotliar and J. Liu, Phys. Rev. Lett. **61**, 1784 (1988).
[33] A.P. Mackenzie, S. R. Julian, A. J. Diver, G. J. McMullan, M. P. Ray, G. G. Lonzarich, Y. Maeno, S. Nishizaki, and T. Fujita, Phys. Rev. Lett. **76**, 3786 (1996).
[34] I.I. Mazin and D.J. Singh, Phys. Rev. Lett. **79**, 733 (1997).